Intrinsic and dynamically generated scalar meson states

C. M. Shakin* and Huangsheng Wang
Department of Physics and Center for Nuclear Theory, Brooklyn College of the City University of New York, Brooklyn, New York 11210
(Received 12 June 2000; published 11 December 2000)

Recent work by Maltman has given us confidence that our assignment of scalar meson states to various nonets based upon our generalized Nambu–Jona-Lasinio (NJL) model is correct. [For example, in our model the $a_0(980)$ and the $f_0(980)$ are in the same nonet as the $K_0^*(1430)$.] In this work we make use of our model to provide a precise definition of ''preexisting'' resonances and ''dynamically generated'' resonances when considering various scalar mesons. [This distinction has been noted by Meissner in his characterization of the $f_0(400-1200)$ as nonpreexisting.] We define preexisting (or intrinsic) resonances as those that appear as singularities of the $q\bar{q}$ T matrix and are in correspondence with $q\bar{q}$ states bound in the confining field. [Additional singularities may be found when studying the T matrices describing π-π or π-K scattering, for example. Such features may be seen to arise, in part, from t-channel and u-channel ρ exchange in the case of π-π scattering, leading to the introduction of the $\sigma(500-600)$. In addition, threshold effects in the $q\bar{q}$ T matrix can give rise to significant broad cross section enhancements. The latter is, in part, responsible for the introduction of the $\kappa(900)$ in a study of π-K scattering, for example.] We suggest that it is only the *intrinsic* resonances which correspond to $q\bar{q}$ quark-model states, and it is only the intrinsic states that are to be used to form quark-model $q\bar{q}$ nonets of states. [While the $\kappa(900)$ and $\sigma(500-600)$ could be placed in a nonet of dynamically generated states, it is unclear whether there is evidence that requires the introduction of other members of such a nonet.] In this work we show how the phenomena related to the introduction of the $\sigma(500-600)$ and the $\kappa(900)$ are generated in studies of π-π and π-K scattering, making use of our generalized Nambu–Jona-Lasinio model. We also calculate the decay constants for the a_0 and K_0^* mesons and compare our results with those obtained by Maltman. We find that the value obtained using QCD sum-rule techniques for the $a_0(980)$ decay constant is smaller than the decay constant calculated using our generalized NJL model, which suggests that the $a_0(980)$ may have a significant $K\bar{K}$ component. We find rather good agreement with Maltman's values for the decay constants of the $a_0(1450)$ and $K_0^*(1430)$. Maltman suggests that the $a_0(980)$ and $K_0^*(1430)$ should be in the same nonet, a result in agreement with our analysis.

DOI: 10.1103/PhysRevD.63.014019 PACS number(s): 14.40.−n, 12.39.Fe

I. INTRODUCTION

In the case of scalar mesons the assignment of the observed resonances to quark-model configurations is problematic. For example, one may identify either the $\sigma(500-600)$, the $f_0(980)$, or the $f_0(1370)$ with the $1\ ^3P_0\ \ n\bar{n}$ state. The latter choice arises if one dismisses the $f_0(980)$ as a $K\bar{K}$ molecule [1] or a $q\bar{q}q\bar{q}$ state [2]. If one chooses the $f_0(1370)$ to be the $1\ ^3P_0\ \ n\bar{n}$ state, the $f_J(1710)$ could be the $1\ ^3P_0\ \ s\bar{s}$ state, with the $f_0(1500)$ having a large glueball component. Without an underlying dynamical model, there exist a broad range of options.

Black, Fariborz, Sannino, and Schechter have made extensive studies of the scalar nonet of states [3–7]. In their recent study of the isovector scalar states [7], Black, Fariborz, and Schechter place the $a_0(980)$, $\kappa(900)$, $f_0(980)$, and the $\sigma(500-600)$ in the nonet of lowest energy, with the $a_0(1450)$ in the same nonet as the $K_0^*(1430)$. The last choice creates a series of problems related to the observed energies of these resonances. [For example, one would expect the $K_0^*(1430)$ to be more massive than the $a_0(1450)$, since the $K_0^*(1430)$ contains a strange quark.] To resolve such problems, these authors introduce two additional states with the quantum numbers of the $a_0(980)$ and $K_0^*(1430)$. (These additional states could be of $q\bar{q}q\bar{q}$ character.) The physical $a_0(980)$ and $K_0^*(1430)$ then arise upon mixing of the $q\bar{q}$ states and the $q\bar{q}q\bar{q}$ states [7].

In their description of quarkonium-glueball mixing Lee and Weingarten [8,9] and Close and Kirk [10] choose the $f_0(1370)$ as the $1\ ^3P_0\ \ n\bar{n}$ state. Close and Kirk place the bare glueball at 1434 MeV and configuration mixing then distributes the bare state, more or less equally, in the physical $f_0(1500)$ and $f_0(1710)$ resonances. Lee and Weingarten choose a larger value for the bare glueball mass so that, upon mixing, the main glueball component is in the $f_0(1710)$, with the $f_0(1500)$ resonance having the largest component of the $1\ ^3P_0\ \ s\bar{s}$ state. Other attempts to understand the scalar meson spectrum may be found if one surveys the extensive references given in Ref. [7].

In our study of the isovector [11] and isoscalar [12] scalar $q\bar{q}$ states we obtained the nonets shown in Figs. 1 and 2. In this work we introduce some evidence to support our analysis. We also show how the $\sigma(500-600)$ and $\kappa(900)$ are generated dynamically. In our model the $a_0(980)$ and $f_0(980)$ are the intrinsic scalar states of lowest energy.

*Email address: casbc@cunyvm.cuny.edu

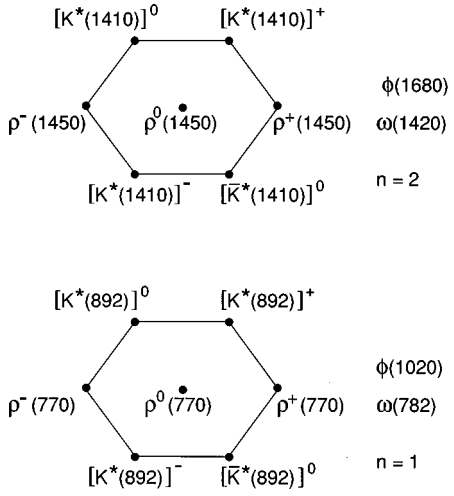

FIG. 1. The nonets of $1\ ^3S_1$ and $2\ ^3S_1$ vector meson states obtained in Ref. [11] are shown.

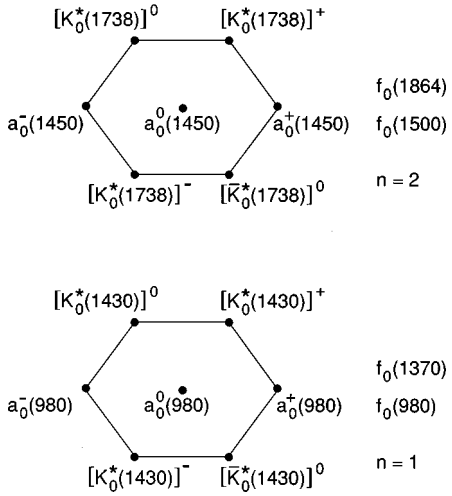

FIG. 2. The nonets of $1\ ^3P_0$ and $2\ ^3P_0$ scalar meson states obtained in Refs. [11] and [12] are shown. The $f_0(1864)$ and $K_0^*(1738)$ are predictions of our analysis with the $f_0(1864)$ being the $2\ ^3P_0\ s\bar{s}$ state. [The properties of the scalar-isoscalar states are modified when we consider quarkonium-glueball mixing. In Ref. [12] we identified the $f_0(1770)$ as the state with the maximum glueball component after such mixing. A covariant model of quarkonium-glueball mixing is presented in Ref. [13].]

The Lagrangian of our model is [11,12]

$$\mathcal{L}=\bar{q}(i\partial-m^0)q+\frac{G_s}{2}\sum_{i=0}^{8}[(\bar{q}\lambda^i q)^2+(\bar{q}^\dagger\gamma_5\lambda^i q)^2]$$
$$-\frac{G_V}{2}\sum_{i=0}^{8}[(\bar{q}\gamma^\mu\lambda^i q)^2+(\bar{q}\gamma^\mu\gamma_5\lambda^i q)^2]$$
$$+\frac{G_D}{2}\{\det[\bar{q}(1+\gamma_5)q]+\det[\bar{q}(1-\gamma_5)q]\}$$
$$+\mathcal{L}_{\rm tensor}+\mathcal{L}_{\rm conf}. \tag{1.1}$$

Here, the fourth term is the 't Hooft interaction, $\mathcal{L}_{\rm tensor}$ denotes interactions added to study tensor mesons, while $\mathcal{L}_{\rm conf}$ denotes our model of confinement [11,12]. In Eq. (1.1) m^0 is the current quark mass matrix $m^0=\mathrm{diag}(m_u^0,m_d^0,m_s^0)$, the $\lambda_i(i=1,...8)$ are the Gell-Mann matrices, and $\lambda_0=\sqrt{2/3}\mathbb{I}$, with $\mathbb{I}$ being the unit matrix in flavor space. In our previous work we had $G_S=11.83\,\mathrm{GeV}^{-2}$ and $G_D=86.39\,\mathrm{GeV}^{-2}$ [11]. The interaction strength in singlet states was $G_{00}=10.46\,\mathrm{GeV}^2$ and the interaction strength in octet states was $G_{88}=12.46\,\mathrm{GeV}^{-2}$. (The nonzero value of G_D induces some small deviations from ideal mixing [12].) If we go to a basis of $n\bar{n}$ and $s\bar{s}$ states, we find $G_{n\bar{n}}=11.12\,\mathrm{GeV}^{-2}$, $G_{s\bar{s}}=11.84\,\mathrm{GeV}^{-2}$ and $G_{n\bar{s}}=-0.94\,\mathrm{GeV}^{-2}$. [See Eq. (4.28) of Ref. [12].] A more recent study, using an improved calculational scheme in the analysis of the $K(495)$, leads to the values $G_{88}=13.10\,\mathrm{GeV}^2$ and $G_{00}=11.10\,\mathrm{GeV}^{-2}$. Results for meson decay constants and for the spectrum of the f_0 mesons presented later in this work are based upon the most recent values of G_{88} and G_{00} that were given above.

In Fig. 3 we show diagrammatic representations of the polarization functions $J_S(P^2)$ and $K_S(P^2)$ that play an important role in our model. [Note that $J_S(P^2)$ is of order n_c and $K_S(P^2)$ of order 1.] In the figure the filled regions denote confinement vertex functions of our model which serve to eliminate (unphysical) singularities that would arise when the quark and antiquark go on mass shell in a theory without confinement [11,12]. Thus, our function $J_S(P^2)$ is real. However, $K_S(P^2)$ is complex, since the mesons appearing in Fig. 3 can go on mass shell. Values calculated for $J_S(P^2)$ for $n\bar{n}$ states are shown in Fig. 4 and values calculated when both quarks are strange are given in Fig. 5. The case where only one quark is strange corresponds to the function $J^S_{u\bar{s}}(P^2)$ shown in Fig. 6. The expression for $J_S(P^2)$ is fairly simple in the case of $n\bar{n}$ states with $m_u=m_d$. If $\vec{P}=0$, we have [11]

$$J_S(P^2)=-4n_c\int\frac{d^3k}{(2\pi)^3}\frac{k^2}{E^2(\bar{k})}\left[\frac{\Gamma_S^{+-}(P^0,k)}{P^0-2E(\bar{k})}-\frac{\Gamma_S^{-+}(-P^0,k)}{P^0+2E(\bar{k})}\right]e^{-\bar{k}^2/\alpha^2} \tag{1.2}$$

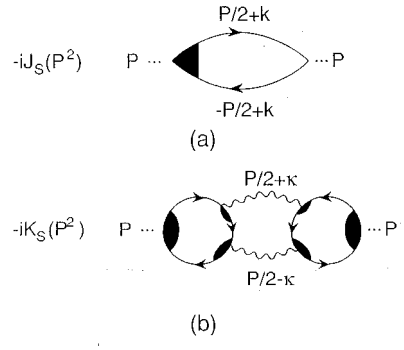

FIG. 3. (a) The leading vacuum polarization diagram of the NJL model is shown. The filled region denotes the confinement vertex function [11,12]. (b) The vacuum polarization diagram that describes coupling to two-meson continuum states. Since the mesons may go on mass shell, $K_S(P^2)$ is complex above the threshold for two-meson decay.

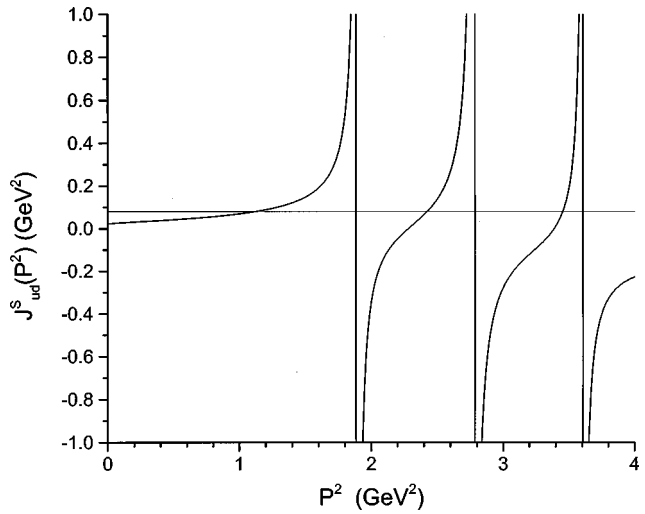

FIG. 4. The function $J^S_{ud}(P^2)$ is shown. The singularities of this function arise from the singularities of the confinement vertex function, which has singularities at the energies of the bound states in the confining field. The figure shows the singularities arising from the $1\ ^3P_0$, $2\ ^3P_0$, and $3\ ^3P_0 n\bar{n}$ states. These states may be put into correspondence with the first three resonances seen in Fig. 8. Here the TDA was used. See Ref. [16] for the result of an RPA calculation.

$$= -4n_C \int \frac{d^3k}{(2\pi)^3}\left[\frac{\overline{k}^2}{E^2(\overline{k})}\right]\Gamma_S^{+-}(P^0,|\overline{k}|) \times\left[\frac{1}{P^0-2E(\overline{k})}-\frac{1}{P^0+2E(\overline{k})}\right]e^{-\overline{k}^2/\alpha^2}, \qquad (1.3)$$

where we have used the fact that $\Gamma_S^{-+}(-P^0,k)$ $=\Gamma_S^{+-}(P^0,k)$ to write Eq. (1.3). The confinement vertex functions, $\Gamma_S(P,k)$, are defined in Ref. [11]. The more complex expressions obtained for unequal quark masses are also given in that work. In Eqs. (1.2) and (1.3) the exponential factor is a Gaussian regulator. In this and previous studies, we have used $\alpha = 0.605$ GeV.

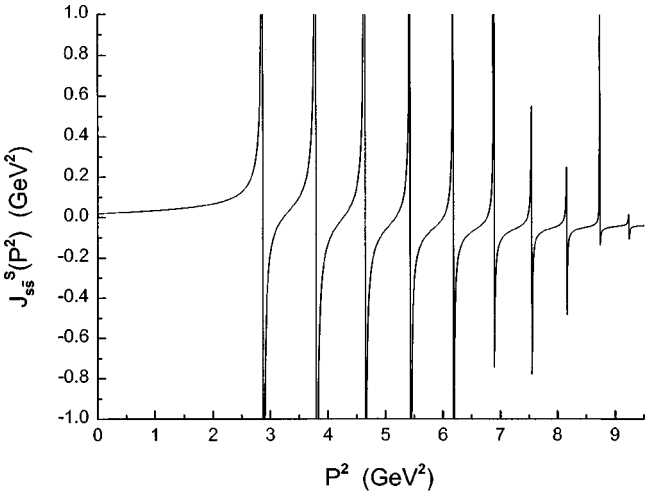

FIG. 5. The figure shows $J^S_{s\bar{s}}(P^2)$. Here both quarks are strange with $m_s = 565$ MeV. There are bound states in the confining field at 1693, 1945, 2154, 2331, 2485, 2625, 2744, 2855, 2955, and 3039 MeV. (We have used a model that is not absolutely confining, such that the continuum starts at $2m_s + V_{\max} = 3150$ MeV [12].) Here the TDA was used. See Ref. [16] for the result of an RPA calculation of $J^S_{s\bar{s}}(P^2)$.

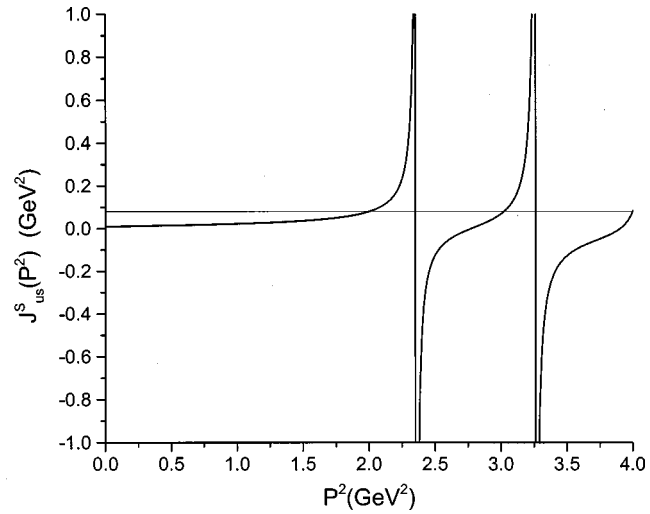

FIG. 6. The function $J^S_{us}(P^2)$ is shown. The singularities are at the energies of the $1\ ^3P_0$ and $2\ ^3P_0$ states which are bound in the confining field. To obtain the mass of the $K_0^*(1430)$ we may consider the intersection of the curve with the line drawn at $G_{88}^{-1} = 0.0802$ GeV. We obtained an energy of 1416 for the mass of the $K_0^*(1430)$, when we neglected $\mathrm{Re}\, K_S^{\pi K}$ in Eq. (2.3) [11]. Here the TDA was used in the calculation of $J^S_{us}(P^2)$.

The organization of our work is as follows. In Sec. II we review some aspects of our generalized Nambu–Jona-Lasinio (NJL) model that are needed for the following discussion. In Sec. III we discuss the work of Maltman concerning the decay constants of the $a_0(980)$ and $K_0^*(1430)$. We also present the results of a calculation of these constants made in our model. In Sec. IV we describe the dynamics that gives rise to the $f_0(400-1200)$ and to the $\kappa(900)$. We argue that these states are not intrinsic states, but are generated dynamically. We also compare our results for the π-π and π-K phase shifts with the experimental data. Finally, Sec. V contains some further discussion and conclusions.

II. A GENERALIZED NAMBU–JONA-LASINIO MODEL

One method for studying the generalized NJL model is to consider the properties of the $q\bar{q}$ T matrix [11,12]. In the case of a single channel, we obtain the form

$$t(P^2) = -\frac{G_s}{1-G_S[J_S(P^2)+\mathrm{Re}\, K_s(P^2)]-iG_S\,\mathrm{Im}\, K_s(P^2)}. \qquad (2.1)$$

(See Fig. 7.) It is useful to write Eq. (2.1) as

$$t(P^2) = -\frac{1}{G_s^{-1}-[J_S(P^2)+\mathrm{Re}\, K_S(P^2)]-i\,\mathrm{Im}\, K_S(P^2)}. \qquad (2.2)$$

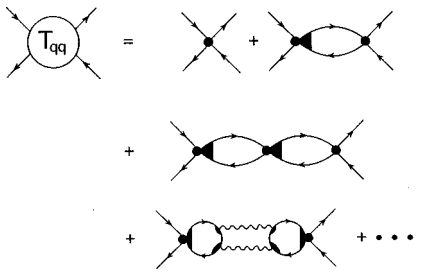

FIG. 7. A perturbation expansion of a $q\bar{q}$ T matrix of our model is shown. Here we have not shown the vertex functions that implement confinement for the initial and final $q\bar{q}$ states. That matter is discussed in detail in Ref. [33], where it is shown that the T matrix is represented only in terms of bound states in a theory with absolute confinement.

To find the meson masses, we solve the equation

$$G_S^{-1}-[J_S(P^2)+\mathrm{Re}\,K_S(P^2)]=0. \tag{2.3}$$

For an isolated resonance, we may consider an expansion about the value $P^2=m_R^2$ obtained from the solution of Eq. (2.3):

$$J_S(P^2)+\mathrm{Re}\,K_S(P^2)=J_S(m_R^2)+\mathrm{Re}\,K_S(m_R^2)+(P^2-m_R^2)\times\left[\frac{\partial J_S(P^2)}{\partial P^2}+\frac{\partial\,\mathrm{Re}\,K_S(P^2)}{\partial P^2}\right]_{P^2=m_R^2}+\cdots. \tag{2.4}$$

With the definition

$$\frac{1}{g^2}=\left[\frac{\partial J_S(P^2)}{\partial P^2}+\frac{\partial\,\mathrm{Re}\,K_S(P^2)}{\partial P^2}\right]_{P^2=m_R^2}+\cdots \tag{2.5}$$

we write Eq. (2.2) as

$$t(P^2)\simeq-\frac{g^2}{P^2-m_R^2+im_R\Gamma_R}, \tag{2.6}$$

where

$$m_R\Gamma_R=g^2\,\mathrm{Im}\,K_S(m_R^2). \tag{2.7}$$

We can generalize this formalism to the multichannel case, as was done in Refs. [11], [12]. There, we obtained the T matrix for π-π and K-$\bar{K}$ scattering in the $I=0$ channels. In the π-π case we took into account the $\pi\pi$, $K\bar{K}$, $\eta\eta$ and $\eta\eta'$ channels. However, the $\eta\eta$ and $\eta\eta'$ channels were weakly coupled, so we presented our results for only the coupled $\pi\pi$ and $K\bar{K}$ channels. We found the values for $|T_{\pi\pi}(E)|^2$ shown in Fig. 8. There we see resonances at $P^0=980$, 1550, 1840, and 2060 MeV. The resonance at 980 MeV is an elastic resonance for which $|T_{\pi\pi}(E)|^2=1$ at the peak. The resonances seen in Fig. 8 have their origin in the $q\bar{q}$ bound states in the confining field. (See Fig. 4.) In Fig. 4, we see singularities at the energies of the $1\ ^3P_0$, $2\ ^3P_0$ and $3\ ^3P_0$ $n\bar{n}$ states that are bound in the confining field. (There are bound states at the energies $P^0=1369$, 1667, 2095, 2262, 2413, 2537 and 2651 MeV, which may be seen in Fig. 3 of Ref. [12].) The states seen in Fig. 8 are obtained when we include the short-range NJL interaction and the effects of $\mathrm{Re}\,K_S(P^2)$ and $\mathrm{Im}\,K_S(P^2)$ in the calculation of $|T_{\pi\pi}(E)|^2$ [12]. These states are in one-to-one correspondence with the states bound in the confining field and are therefore the *intrinsic* states that we have defined at an earlier point of our discussion. In Fig. 8 an enhanced cross section is seen in the region $2m_\pi<E\leqslant 1200$ MeV. We will return to a discussion of that enhancement in Sec. IV, where we discuss the $f_0(400-1200)$ [or $\sigma(500-600)$]. Our result for $|T_{K\bar{K}}(E)|^2$ for the $I=0$ channel was given in Ref. [12]. Those results were recalculated and are shown in Fig. 9. In this case we have reduced the coupling to the $K\bar{K}$ channel in the calculation of $\mathrm{Im}\,K_S^{KK}(P^2)$ to yield more reasonable values for the widths, which were overestimated in Ref. [12]. [The large value of the width of the $f_0(1370)$ found in Ref. [12] was due to an asymmetric treatment of the pion and the kaon. We had neglected confinement for the pion and included it for the kaon. A more symmetric treatment reduces the width of the $f_0(1370)$ from 192 MeV to about 50 MeV, as seen in Fig. 9.] The states at $P^0=1412$, 1855 and 2105 MeV seen in Fig. 9 are *intrinsic* states that arise from the $1\ ^3P_0$, $2\ ^3P_0$ and $3\ ^3P_0$ $s\bar{s}$ states bound in the confining field. These are among the states seen in Fig. 5. The other (small) peaks seen in Fig. 9 arise from deviations from ideal mixing due to the presence of the 't Hooft interaction. They correspond to the intrinsic states already seen in Fig. 8.

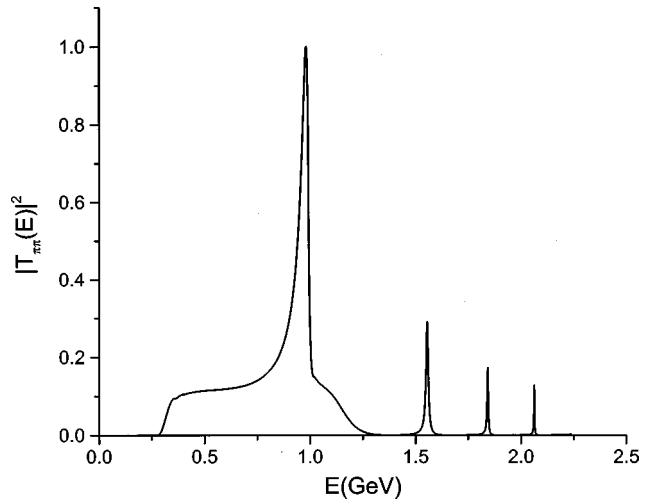

FIG. 8. The values of the squared T matrix for $\pi\pi$ scattering obtained in Ref. [12] are shown. In the absence of inelastic events, the quantity shown is equal to $\sin^2\delta_{00}(E)$. The first peak represents the $f_0(980)$ resonance and the second is the $f_0(1500)$ resonance, which we found at 1550 MeV [12]. [In the case of the $f_0(1500)$, the width is greatly enhanced when we consider the decay to the 4π channel. A discussion of the $\pi\pi$ and $K\bar{K}$ decay widths of the $f_0(1500)$ is given in Ref. [13], where quarkonium-glueball mixing is taken into account in a covariant model.]

A comprehensive study of the spectrum of scalar states above $P^0=1$ GeV requires a treatment of quarkonium-glueball mixing. A covariant treatment of such mixing is

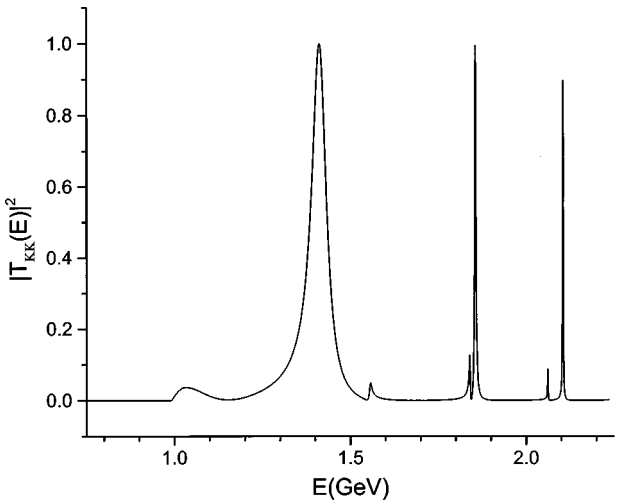

FIG. 9. Values of $|T_{K\bar{K}}(E)|^2$ are shown. These results may be compared to those of Fig. 16 of Ref. [12]. Here we have reduced the values of $\mathrm{Im}\, K_S^{K\bar{K}}(P^2)$ by a factor of four to obtain a reasonable value for the $K\bar{K}$ decay width of the $f_0(1370)$ of 50 MeV. [We believe that the value of $g_{K_{qq}}$ used in Ref. [12] was about 40% too large due to an asymmetric treatment of the pion and the kaon in that work (see the text).] The three small peaks above 1.5 GeV correspond to the three peaks above 1.5 GeV seen in Fig. 8. Their presence represents deviations from ideal mixing.

given in Ref. [13]. (We do not discuss the results of that work, since they are not important for the purposes of the present study.)

III. SCALAR MESON DECAY CONSTANTS

Maltman has argued that we can gain some information concerning the correct assignment of the $a_0(980)$ to a scalar nonet by comparing the decay constants of the $a_0(980)$ and the $K_0^*(1430)$ [14,15]. He remarks that it is natural to put the K meson and the pion into the same octet of Goldstone bosons, since they have decay constants which only differ by about 20%. He also notes that if the $a_0(980)$ were a $K\bar{K}$ molecule, one would expect a quite small decay constant for the $a_0(980)$ relative to the decay constant of the $K_0^*(1430)$, which is believed to be a simple $q\bar{q}$ state. Maltman studies the scalar correlator

$$\Pi(q^2)=i\int d^4x e^{iq\cdot x}\langle 0|T(j(x)j^\dagger(0))|0\rangle, \tag{3.1}$$

with $j^{du}(x)=\partial_\mu(\bar{d}\gamma^\mu u)$ or $j^{su}=\partial_\mu(\bar{s}\gamma^\mu u)$. He then defines

$$-i\langle 0|j^{su}(0)|K_0^*(1430)\rangle=f_{K_0^*(1430)}m^2_{K_0^*(1430)} \tag{3.2}$$

and

$$-i\langle 0|j^{du}(0)|a_0(980)\rangle=\hat{f}_{a_0(980)}m^2_{a_0(980)}. \tag{3.3}$$

In QCD, one has

$$\partial_\mu(\bar{q}^a\gamma^\mu q^b)=i(m_a^0-m_b^0)S^{ab}, \tag{3.4}$$

with $S^{ab}=\bar{q}^a q^b$. It is then useful to define the a_0 decay constant using the relation

$$\left[\frac{m_s-m_u}{m_d-m_u}\right]\langle 0|j^{du}(0)|a_0(980)\rangle=f_{a_0(980)}m^2_{a_0(980)}. \tag{3.5}$$

Multiplication by $(m_s-m_u)/(m_d-m_u)$ leads to a value for the $a_0(980)$ decay constant that is similar to that of the $K_0^*(1430)$, if these states have similar configurations. Without that factor the $a_0(980)$ would have a zero value for the decay constant if $m_u=m_d$. If we consider the mesons of positive charge, we may use

$$-ij^{su}=(m_s^0-m_u^0)\bar{s}u \tag{3.6}$$

$$=(m_s^0-m_u^0)\frac{1}{\sqrt{2}}\bar{q}\left[\frac{\lambda_4-i\lambda_5}{\sqrt{2}}\right]q \tag{3.7}$$

and

$$-ij^{du}=(m_s^0-m_u^0)\frac{1}{\sqrt{2}}\bar{q}\left[\frac{\lambda_1-i\lambda_2}{\sqrt{2}}\right]q. \tag{3.8}$$

Using the expressions given in Eqs. (3.7) and (3.8), we may readily obtain the results for our model. We proceed by constructing the wave functions of the a_0 and K_0^* mesons. Equations may be written for the bound-state amplitudes [16]:

$$\phi_i^*(k)=\frac{\hat{\Gamma}_i^{+-}(k)}{P_i^0-E_a(\bar{k})-E_b(\bar{k})} \tag{3.9}$$

and

$$\phi_i^-(k)=-\frac{\hat{\Gamma}_i^{+-}(k)}{P^0+E_a(\bar{k})+E_b(\bar{k})}, \tag{3.10}$$

where $E_a(k)=[\bar{k^2}+m_a^2]^{1/2}$. Here $\hat{\Gamma}_i^{+-}(k)$ is a vertex function for a bound state (i) that includes the effect of both the NJL interaction and confinement. The amplitudes $\phi_i^+(k)$ and $\phi_i^-(k)$ satisfy coupled equations which are relativistic generalizations of the nonrelativistic random-phase approximation (RPA) calculations made many years ago in the study of particle-hole excitations in nuclei [17]. We may also define Tamn-Dancoff-approximation (TDA) calculations by neglecting $\phi_i^-(k)$ as well as the second term in the brackets appearing in Eqs. (1.2) and (1.3). The details of such calculations are given in Ref. [16]. We present the results of our calculations in Table I, where the theoretical values are compared to those obtained by Maltman, who used QCD sum rules and other methods to obtain the decay constants of the $a_0(980)$, $a_0(1450)$ and $K_0^*(1430)$. Our result for the $a_0(980)$ is about twice Maltman's value which suggests a significant $K\bar{K}$ component in the $a_0(980)$ wave function.

TABLE I. Meson decay constants for the a_0 and K_0^* mesons [16]. (See Figs. 1 and 2.)

		$m_i^2 f_i(\mathrm{GeV}^3)$		
Meson	Configuration	TDA	RPA	Maltman [14,15]
$a_0(980)$	$1\ ^3P_0$	0.0852	0.114	0.0447 ± 0.0085
$a_0(1450)$	$2\ ^3P_0$	0.0469	0.0552	0.0647 ± 0.0123
$a_0(1834)$[a]	$3\ ^3P_0$	0.0495	0.0557	
$K_0^*(1430)$	$1\ ^3P_0$	0.0806	0.0667	0.0842 ± 0.0045
$K_0^*(1738)$[a]	$2\ ^3P_0$	0.0558	0.0492	
$K_0^*(1950)$	$3\ ^3P_0$	0.0544	0.0497	

[a]These states are predicted to exist in our formalism.

Our results for the decay constants of the $a_0(1450)$ and $K_0^*(1430)$ are quite satisfactory when compared to Maltman's values.

As may be seen in Table I, the $a_0(1450)$ and $K_0^*(1430)$ have similar decay constants which might suggest that they belong in the same nonet. However, in our model, which reproduces the experimental energies of the $a_0(980)$, $f_0(980)$, $a_0(1450)$ and $K_0^*(1430)$ quite well, the $a_0(1450)$ is a $2\ ^3P_0$ state and the $K_0^*(1430)$ is a $1\ ^3P_0$ state. Therefore, the assignment of states to nonets in our model must be that seen in Fig. 2. We can conclude from these observations that similar values for meson decay constants is not a sufficient condition for placing meson states in the same nonet. The fact that we do rather well in reproducing Maltman's values of the decay constants serves to provide further evidence that our assignment of scalar states to nonet, based upon the results of our generalized NJL model, is correct.

IV. DYNAMICALLY GENERATED STATES

In this section we wish to describe the origin of the cross section enhancements seen in $\pi\pi$ and πK scattering that lead to the introduction of the $\sigma(500-600)$ and $\kappa(900)$. The results of t-channel and u-channel ρ exchange were used in Ref. [18] to define a K-matrix for $\pi\pi$ scattering with the result that

$$\frac{\tan\delta_{00}(k)}{\rho} = -\frac{g^2}{16\pi}\left[2+\left[\frac{8k^2+4m_\pi^2+m_\rho^2}{2k^2}\right]\ln\left[\frac{m_\rho^2}{4k^2+m_\rho^2}\right]\right], \tag{4.1}$$

with $k=|\overline{k}|$. Here, $g=g_{\rho\pi\pi}\simeq 6.0$,

$$\rho=\left(1-\frac{4m_\pi^2}{P^2}\right)^{1/2}, \tag{4.2}$$

and

$$\overline{k^2}=\frac{P^2}{4}-m_\pi^2. \tag{4.3}$$

The phase shift generated in this manner is shown as a dotted line in Fig. 10. We wish to combine the s-channel phase shift calculated using our generalized NJL model and the phase shift due to ρ exchange. The simplest possible scheme is just to add the phase shifts. The result of that addition is seen as the solid line in Fig. 10. In Fig. 11 we see that this procedure yields a total phase that fits the data quite well, although we are somewhat above the data points in the region below 600 MeV. (The small circles, which represent the values of our calculated total phase shift, are not drawn in the regions where they coincide with the data points.) Although our treatment of the unitarity constraint is oversimplified, our result does suggest that the $f_0(400-1200)$ [or the $\sigma(500-600)$] is a dynamically-generated state in the sense defined above.

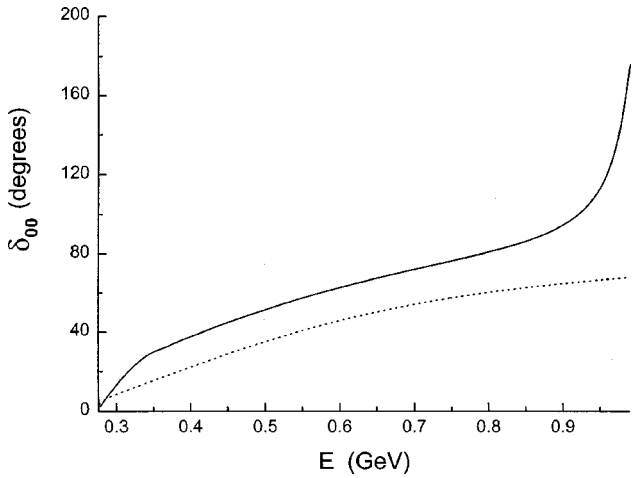

FIG. 10. The phase shift $\delta_{00}(E)$ is shown for the case of t-channel and u-channel ρ exchange (dotted line) [18]. The solid line is the result obtained when the phase shift of our model is added to the phase shift for ρ exchange as calculated in Ref. [18].

We have also performed a similar calculation of the low-energy π-K phase shift. That phase shift is known to be elastic below 1300 MeV. The threshold for the $\eta' K$ channel is at 1453 MeV and the ηK channel is only weakly coupled to the πK channel [19,20]. Again, there are phase shifts of similar size arising from ρ and K^* exchange, and s-channel enhancements of the cross section in our $q\overline{q}$ T matrix. If we

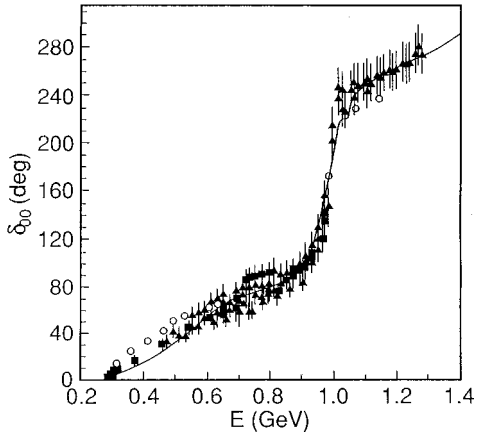

FIG. 11. Experimental values of the δ_{00} phase shift for $\pi\pi$ scattering as complied in Ref. [29] are shown. The small circles represent the values given by the solid curve in Fig. 10.

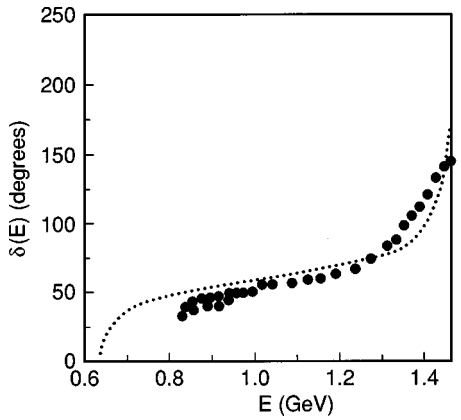

FIG. 12. The experimental values of the π-K scattering phase shift is shown in the region below the $\eta' K$ threshold at 1453 MeV [19]. The dotted line represents the sum of the phase shift calculated for ρ and K^* exchange and the s-channel phase shift of our generalized NJL model. These effects give rise to an enhanced cross section from threshold to the energy of the $K_0^*(1430)$ resonance.

again add the phase shifts and neglect inelasticity, we obtain the dotted curve seen in Fig. 12. We note that the experimental data [19] for the phase shift pass through 90° at about 1300 MeV which reflects the importance of the background amplitude in moving the 90° point to about 100 MeV below the energy of the resonance. [The model described in Ref. [11] places the $K_0^*(1430)$ at 1416 MeV.]

V. CONCLUSIONS AND DISCUSSION

Recently, Cherry and Pennington have performed a model-independent analytic continuation of the πK scattering results below 2 GeV in order to determine the number and position of the resonance poles. They find poles representing the $K_0^*(1430)$ but no pole corresponding to the $\kappa(900)$ [21]. That result might appear to eliminate the model in which one places the $a_0(980)$, $f_0(980)$, $\sigma(500-600)$ and $\kappa(900)$ in an SU3 nonet of states. However, the existence of the $\kappa(900)$ is still a controversial matter. It has been suggested that the procedures used by Cherry and Pennington might not be sufficient to decide this issue. Indeed, a recent analysis of πK scattering in a chiral model with resonances finds a κ meson pole at $708-i305$ MeV. The analysis of scalar meson decay constants made by Maltman suggests that the $a_0(980)$ belongs in the same octet as the $K_0^*(1430)$. For the $a_0(980)$, we find that our calculated value of the decay constant is about twice the value obtained using QCD sum rules. This disagreement probably has its origin in a significant $K\bar{K}$ component of the $a_0(980)$ wave function. However, the overall agreement of the decay constants obtained by different methods suggests that the classification of scalar states shown in Fig. 2 is correct.

We have also described the origin of the enhancements of the cross section in low-energy $\pi\pi$ and $\pi\bar{K}$ scattering that have led to the introduction of the $\sigma(500-600)$ and the $\kappa(900)$, respectively. We have considered t-channel and u-channel ρ exchange in the case of $\pi\pi$ scattering and K^* and ρ exchange in the case of πK scattering. Although our method of implementing unitarity by adding the phase shift obtained in the study of t and u-channel exchange to the s-channel phase shift calculated in our generalized NJL model might be improved upon, the results provide a satisfactory fit to the experimental data. Our model has some relation to that used in Ref. [22]. In that work a chiral model with only meson degrees of freedom is used. Various resonances in the πK system are inserted in a phenomenological manner and t and u-channel exchange of vector meson nonets is considered. On the other hand, in our model, these resonances are generated dynamically when we construct the $q\bar{q}$ T matrix. That construction is supplemented by vector meson exchange in a manner similar to that used in Ref. [22]. Our model has the advantage that the various resonance poles needed to fit the data in Ref. [22] can be separated into three intrinsic states and a single dynamically-generated state which we identify as the $\kappa(900)$. It would be desirable to improve our model of $\pi\pi$ and πK scattering with more attention paid to unitarity and chiral symmetry constraints.

In addition to the work of Maltman [14,15], there have been a number of other attempts to gain information concerning the properties of scalar mesons using QCD sum rules [23,24]. The study of the nonstrange $(n\bar{n})$ scalar sector reported in Ref. [24] suggests that both the $f_0(400-1200)$ and the $a_0(980)$ are not $n\bar{n}$ states. However, Maltman concludes that the $a_0(980)$ is a $n\bar{n}$ state. He explains that the work of Ref. [24] has used a more restrictive single-resonance-plus continuum model for the input spectral function and shows that that form leads to a very poor match between the operator product expansion and the hadronic sides of the sum rule, in contrast to his results [15]. [We agree with Maltman's result that the $a_0(980)$ is a $n\bar{n}$ state, or at least, that it has a large $n\bar{n}$ component.]

There are various opinions put forth in the literature concerning the $f_0(400-1200)$, or $\sigma(500-600)$. For example, Meissner suggests that the $f_0(400-1200)$ is not a ''preexisting'' resonance, but is a dynamic effect due to the strong pion-pion interaction in the $L=0$, $I=0$ wave [25]. He also states that the $f_0(400-1200)$ is certainly not the chiral partner of the pion. Contrasting points of view have been put forth by Pennington [26] and Hatsuda and Kunihiro [27–30].

In general, one may decide whether a meson ''exists'' by looking for poles in the relevant scattering matrix, as was done in Ref. [21]. The conclusion reached in Ref. [21] was that the $\kappa(900)$ does not exist, however, that result is not conclusive. On the other hand, there does appear to be a pole associated with the $\sigma(500-600)$ [31–33]. In our work we have stressed that, if one has an underlying dynamical model, some of these poles may be related to $q\bar{q}$ states (or more complex states) of a chiral quark model, such as our generalized NJL model [35]. The poles that have that correspondence are associated with *intrinsic* states and other poles with *dynamically-generated* states. From this point of view, the existence of the $\kappa(900)$ is somewhat irrelevant, since it would be a dynamically-generated state in our model and, therefore, not a member of a SU3 quark-model nonet.

Finally, in Fig. 13, we show the relation between the states bound in the confining field and the intrinsic states of

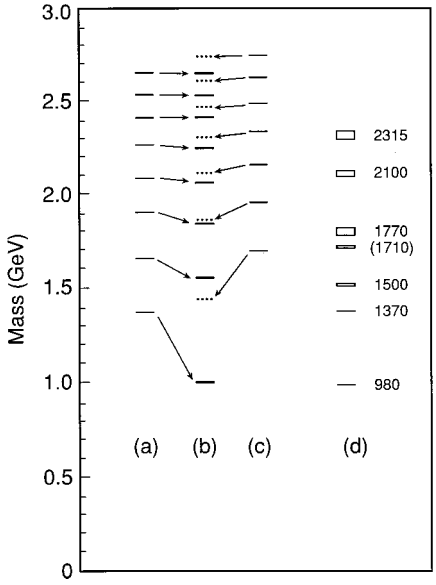

FIG. 13. This figure is taken from Ref. [34]. Column (a) shows the $n\bar{n}$ states bound in the confining field and column (c) shows the $s\bar{s}$ states. The inclusion of the short-range NJL interaction and some dispersive effects described by $K_S(P^2)$ results in the energies of the *intrinsic* states shown in column (b). Column (d) shows the experimental spectrum of f_0 resonances.

our model in the case of the f_0 mesons [12]. Columns (a) and (c) show the $n\bar{n}$ and $s\bar{s}$ states bound in the confining field. The introduction of the short-range NJL interaction then generates the *intrinsic* states of column (b). [The energies of the intrinsic states are also modified somewhat by various dispersive effects described by $K_S(P^2)$ [12].] The resulting intrinsic spectrum of column (b) may be compared to the experimental spectrum of f_0 states shown in column (d).

When calculating the energies shown in columns (a), (b) and (c), parameters that were previously fixed were used, so that these results may be considered predictions of the previously constructed model Lagrangian. If we assume that the spectrum of f_0 mesons may be obtained using parameters determined in the study of the pseudoscalar and vector nonets, we find that the $f_0(980)$ is the isoscalar $q\bar{q}$ state of lowest energy. It is clear from this analysis that, in our model, the $\sigma(500-600)$ must be identified as a *dynamically-generated* state, in accordance with our previous discussion.

The distinction that we have made between intrinsic and dynamically-generated states is model dependent, but has the advantage that there is an underlying quark model that in itself is related to meson spectroscopy based upon the identification of quark configurations. The identification of intrinsic and dynamically-generated states is a different matter in a theory of meson-meson scattering based upon the use of chiral Lagrangians, supplemented by a unitarization scheme. For example, in Ref. [33] it is stated that ''the $a_0(980)$, σ and $\kappa(900)$ resonances are meson-meson states originating from the unitarization of the $O(P^2)$ χPT amplitude. On the other hand, the $f_0(980)$ is a combination of a strong S-wave meson-meson unitarity effect and a preexisting singlet resonance with a mass around 1 GeV.'' We believe further work is required to understand the relation between ''dynamically generated'' states as defined in Ref. [33] and the definition we have put forth in this work.

ACKNOWLEDGMENTS

This work was supported in part by a grant from the National Science Foundation and by the PSC-CUNY Faculty Award Program.

[1] J. Weinstein and N. Isgur, Phys. Rev. Lett. **48**, 659 (1982); G. Jannsen, B. C. Pierce, K. Holinde, and J. Speth, Phys. Rev. D **52**, 2690 (1995).
[2] R. Jaffe, Phys. Rev. D **15**, 281 (1977).
[3] M. Harada, F. Sannino, and J. Schechter, Phys. Rev. D **54**, 1991 (1996).
[4] F. Sannino and J. Schechter, Phys. Rev. D **52**, 96 (1995).
[5] D. Black, A. H. Fariborz, F. Sannino, and J. Schechter, Phys. Rev. D **58**, 054012 (1998).
[6] D. Black, A. H. Fariborz, F. Sannino, and J. Schechter, Phys. Rev. D **59**, 074026 (1999).
[7] D. Black, A. H. Fariborz, and J. Schechter, Phys. Rev. D **61**, 074001 (2000).
[8] W. Lee and D. Weingarten, Nucl. Phys. B (Proc. Suppl.) **73**, 249 (1999); D. Weingarten, *ibid.* **53**, 232 (1997).
[9] W. Lee and Weingarten, Phys. Rev. D **59**, 094508 (1999).
[10] F. E. Close and A. Kirk, Phys. Lett. B **483**, 345 (2000).
[11] L. S. Celenza, Bo Huang, Huangsheng Wang, and C. M. Shakin, Phys. Rev. C **60**, 025202 (1999).
[12] L. S. Celenza, Shun-fun Gao, Bo Huang, Huangsheng Wang, and C. M. Shakin, Phys. Rev. C **61**, 035201 (2000).
[13] L. S. Celenza, Bo Huang, Huangsheng Wang, and C. M. Shakin, Brooklyn College Report No. BCCNT 99/111/283R3 (1999).
[14] K. Maltman, Phys. Lett. B **462**, 14 (1999).
[15] K. Maltman, Scalar Decay Constants and the Nature of the $a_0(980)$, presented at the International Conference on Quark Nuclear Physics, Adelaide, 2000, hep-ph/0005155.
[16] C. M. Shakin and Huangsheng Wang, Brooklyn College Report No. BCCNT 00/091/295 (2000).
[17] A. L. Fetter and J. D. Walecka, *Quantum Theory of Many-Particle Systems* (McGraw-Hill, New York, 1971) (see Chap. 15).
[18] B. S. Zou and D. V. Bugg, Phys. Rev. D **50**, 591 (1994).
[19] LASS Collaboration, D. Aston *et al.*, Nucl. Phys. **B296**, 493 (1988).
[20] N. A. Törnqvist, Z. Phys. C **68**, 647 (1995).
[21] S. N. Cherry and M. R. Pennington, ''There is no $\kappa(900)$,'' arXiv: hep-ph/0005208, 2000.
[22] M. Jamin, J. A. Oller, and A. Pich, arXiv: hep-ph/0006045, 2000.
[23] V. Elias, A. H. Fariborz, Fang Shi, and T. G. Steele, Nucl. Phys. **A633**, 279 (1998).
[24] F. Shi, T. G. Steele, V. Elias, K. B. Speaque, Ying Xue, and A.

H. Fariborz, Nucl. Phys. **A671**, 416 (2000).
[25] Ulf-G. Meissner, Contribution to the III Workshop on Physics and Detectors for DAΦNE, Frascati, 1999, hep-ph/0001066.
[26] M. R. Pennington, presented at the Workshop on Hadron Spectroscopy (WHS99), Frascati, 1999, hep-ph/9905241.
[27] T. Hatsuda and T. Kunihiro, Phys. Rep. **247**, 221 (1994).
[28] T. Kunihiro and T. Hatsuda, Phys. Lett. B **240**, 209 (1990).
[29] T. Hatsuda, Phys. Rev. Lett. **65**, 543 (1990).
[30] T. Kunihiro, Invited talk presented at the Workshop on Hadron Spectroscopy (WHS99), Frascati, 1999, hep-ph/9905262.
[31] T. Hannah, Phys. Rev. D **60**, 017502 (1999).
[32] J. A. Oller, E. Oset, and J. R. Pelaez, Phys. Rev. D **59**, 074001 (1999); **59**, 099906(E) (1999).
[33] J. A. Oller and E. Oset, Phys. Rev. D **60**, 074023 (1999).
[34] L. S. Celenza, Bo Huang, and C. M. Shakin, Phys. Rev. C **59**, 1030 (1999).
[35] C. M. Shakin and Huangsheng Wang, Brooklyn College Report No. BCCNT 00/081/294 (2000).